tvst

Glaucoma

Age-Related Changes in Dynamic Iris Behavior Assessed Using a Programmable Closed-Loop Iris Control System

Galo Apolo[1], Naim Lazkani[1], Sarah Zhou[2], Abe E. Song[1], Anmol A. Pardeshi[1], Lernik Torossian[1], Kent Nguyen[1], Robert N. Weinreb[3], and Benjamin Y. Xu[1]

[1] Roski Eye Institute, Department of Ophthalmology, Keck School of Medicine at the University of Southern California, Los Angeles, CA, USA
[2] Keck School of Medicine at the University of Southern California, Los Angeles, CA, USA
[3] Hamilton Glaucoma Center, Shiley Eye Center and Viterbi Family Department of Ophthalmology, University of California, San Diego, La Jolla, CA, USA

Correspondence: Benjamin Xu, Department of Ophthalmology, Keck School of Medicine at the University of Southern California, 1450 San Pablo Street, 4th Floor, Suite 4700, Los Angeles, CA 90033, USA. e-mail: benjamin.xu@med.usc.edu

Received: May 23, 2022
Accepted: October 8, 2022
Published: November 14, 2022

Keywords: angle closure; glaucoma; iris behavior; iris control

Citation: Apolo G, Lazkani N, Zhou S, Song AE, Pardeshi AA, Torossian L, Nguyen K, Weinreb RN, Xu BY. Age-related changes in dynamic iris behavior assessed using a programmable closed-loop iris control system. Transl Vis Sci Technol. 2022;11(11):9, https://doi.org/10.1167/tvst.11.11.9

Purpose: The purpose of this study was to develop and test a programmable closed-loop system for tracking, modulating, and assessing dynamic iris behavior, including in the mid-dilated position.

Methods: A programmable closed-loop iris control system was developed by customizing an ANTERION OCT device (Heidelberg Engineering, Heidelberg, Germany). Custom software was developed to store camera and optical coherence tomography (OCT) images, track pupillary diameter (PD), control a light-emitting diode (LED), and modulate ambient lighting to maintain the iris in a dilated, constricted, or mid-dilated position in real-time. Study participants underwent 3 consecutive 65-second scan sessions. Dynamic iris behavior in the form of peak constriction velocity (PCV) and mid-dilated iris activity (MDIA) were calculated and analyzed offline.

Results: Among 58 participants, 56 (96.6%) were eligible for analysis based on achieving and maintaining mean PD within ±10% of the calculated mid-dilated PD. Mean participant age was 49.8 ± 18.9 years. Mean PCV was 3.92 ± 0.83 mm/s, and mean MDIA was 0.37 ± 0.15 mm. The mean difference between the calculated and achieved mid-dilated PD was 0.166 ± 0.192 mm. There were significant negative correlations between PCV and age (slope = −0.022, $P < 0.001$) and MDIA and age (slope = −0.004, $P < 0.001$). Success rates were lower (69.0%) but relationships between dynamic iris behavior and age were similar based on achieving and maintaining mean PD within ±5% of the calculated mid-dilated PD.

Conclusions: A programmable closed-loop iris control system can modulate dynamic iris behavior and maintain the iris in a mid-dilated position. Pupillary constriction velocity and iris activity in the mid-dilated position decrease with age.

Translational Relevance: This system can be applied to study dynamic disease processes involving the iris and establish novel biometric measures that could serve as risk factors for acute and chronic primary angle closure glaucoma (PACG).

Introduction

The iris is an ocular anatomic structure that dynamically changes size, position, and configuration in response to a range of physiologic stimuli, including changes in ambient lighting.[1] Biometric parameters describing the iris, such as iris curvature, area, and thickness, are determinants of anterior chamber angle width and associated with increased risk of angle closure on gonioscopy.[2–6] Whereas the iris appears to play a central role in anterior segment biometry and pathogenesis of primary angle closure disease (PACD), static iris parameters alone appear insufficient for predicting which patients will develop severe PACD, including primary angle closure glaucoma (PACG).[7] This is especially true for predicting rare but devastating dynamic angle closure events, such as acute primary angle closure (AAC) attacks, that confer high risk of glaucomatous damage. Therefore, there is a compelling

need to study the role of dynamic iris behavior for risk-stratifying eyes for PACG.

Recent research has focused on dynamic iris behavior induced by changes in ambient lighting that could contribute to anatomic mechanisms of PACD. Iris volume changes with pupillary constriction or dilation due to permeability of iris tissue to aqueous humor.[8] A smaller reduction in iris volume during pupillary dilation is a risk factor for AAC and PACG, possibly due to obstruction of the trabecular meshwork (TM) by peripheral iris tissue.[8] Pupillary block is another dynamic anatomic process that plays an important role in angle closure. Pupillary block results from close apposition between the posterior surface of the iris and anterior surface of the lens leading to increased resistance to aqueous flow from the posterior to the anterior chamber through the pupil.[9] As aqueous humor accumulates in the posterior chamber, and the iris is pushed forward toward the TM. The amount of iris-lens contact differs between the light and dark, which may explain why AAC is triggered under specific environmental conditions, including dim lighting.[10] However, there are currently no convenient methods to study anatomic changes and dynamic behavior of the iris in the mid-dilated position, which is believed to confer the greatest risk of AAC.[11]

In this study, we develop a novel programmable closed-loop iris control system for modulating and assessing dynamic behavior of the iris in various positions, including the mid-dilated position. This system is more flexible and customizable compared with previous methods for studying dynamic iris behavior, which relied on images or videos of the iris under static or transitioning between bright and dark lighting conditions.[1,8,12-14] We also test our system by characterizing age-related changes in dynamic iris behavior, including iris activity in the mid-dilated position.

Methods

The study was approved by the University of Southern California (USC) Institutional Review Board. All study procedures adhered to the recommendations of the Declaration of Helsinki. Written informed consent was obtained from all participants.

Study Participants

Participants 18 years of age and older undergoing routine eye examinations were recruited from eye clinics at the USC Roski Eye Institute. Recruitment occurred between March 2021 and August 2021. Participants with a medical history of intraocular surgery or with evidence of disease were excluded. Eyes receiving medications or drops that could affect iris behavior were also excluded. If both eyes of a participant were eligible, one eye was selected at random for imaging and analysis.

Materials and System Development

A custom programmable closed-loop iris control system was designed and developed to track and modulate dynamic behavior of the iris. The system had four primary components: (1) the ANTERION OCT system (Heidelberg Engineering, Heidelberg, Germany); (2) an ARDUINO UNO board (Arduino LLC, Somerville, MA, USA); (3) a custom graphical user interface (GUI) and data storage program coded in MATLAB (version R2021a; Mathworks, Natick, MA, USA) running on the ANTERION's computer unit; and (4) a single light emitting diode (LED) with maximum voltage input of 5 volts (V) and luminance output of 890 lux (Fig. 1). The LED was positioned above the objective lens of the ANTERION at 7 cm from the imaging plane with an angle of elevation of 45 degrees (see Fig. 1).

The MATLAB GUI prompted the user to input participant information (study identification number, age, and eye scanned) prior to the start of each of scan session. It also showed a real-time plot of the pupillary diameter (PD) throughout each scan session. The system was designed to act as a closed-loop circuit that adjusted voltage output and LED intensity based on the measured PD. The maximum voltage delivered to the LED during each scan session was limited to 4 V, corresponding to a luminance of 710 lux at the imaging plane (Dr. Meter Digital Illuminance Meter, model-LX1330B, California, USA), to avoid participant discomfort.

Data Acquisition

Data acquisition was performed in a dark room under standardized lighting conditions (<0.01 lux) at the imaging plane. Participants were scanned while in the seated position and were instructed to maintain fixation on the ANTERION's internal fixation target. The refractive error of the fixation target was set at +1.00 diopters (D) to relax accommodation and minimize its effect on PD. The room lights were turned off and the participant waited no more than 60 seconds in the dark before starting each scan session to limit the effects of dark adaptation on iris behavior. Each eye was scanned 3 times; each scan session lasted 65 seconds. The time between each scan was between 15 and 60 seconds to allow participants to relax their eyes.

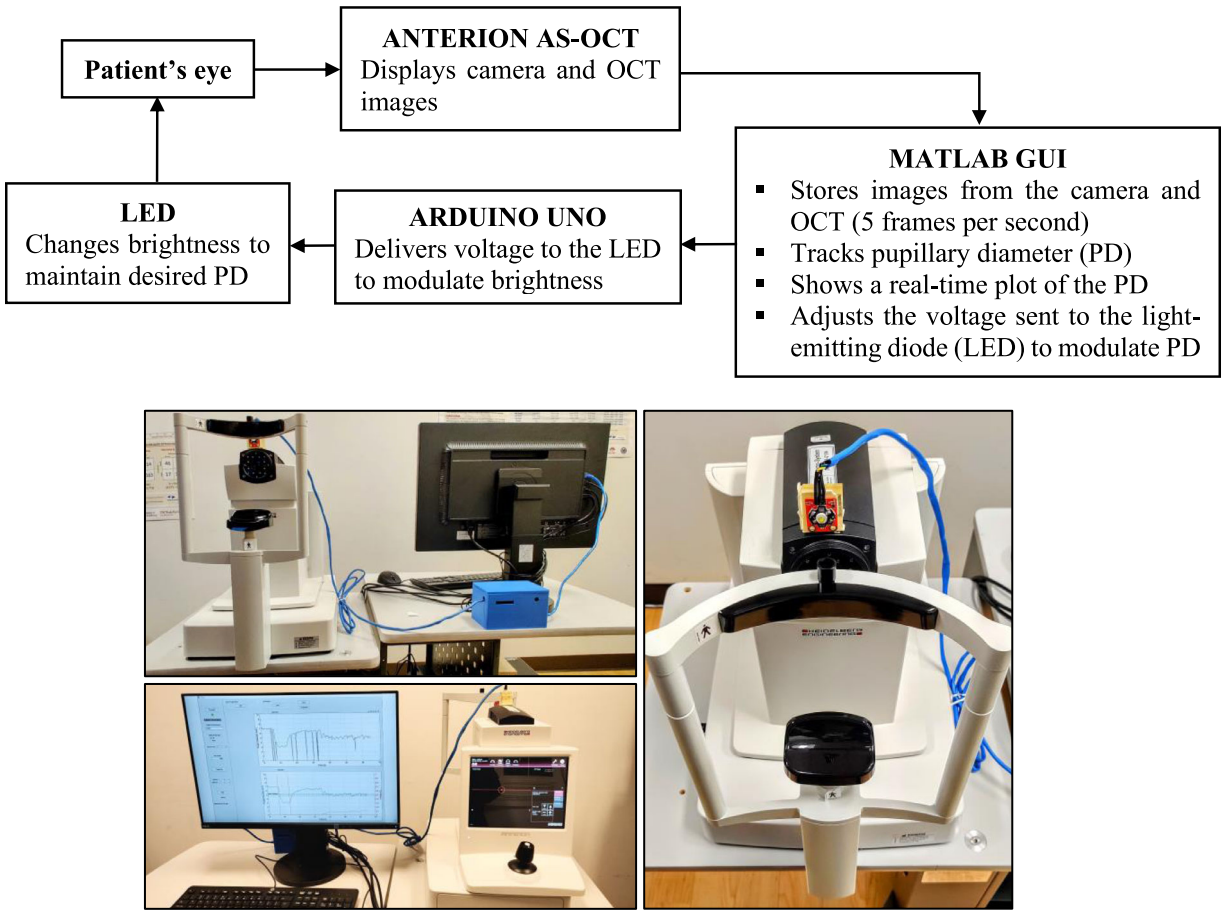

Figure 1. Block diagram and photos of the programmable closed-loop iris control system.

Each scan session consisted of tracking and modulating the PD while adjusting the LED intensity to achieve and maintain the mid-dilated pupillary diameter (MidPD), defined as the average of maximum PD (MaxPD) and minimum PD (MinPD). The sequence of each scan session was: (1) during the first 7 seconds of each scan session, all room and system lights were OFF (<0.01 lux at the imaging plane) and MaxPD was measured; (2) the LED above the objective lens of the ANTERION was turned ON (approximately 710 lux at the imaging plane) for the next 7 seconds and MinPD was measured; (3) the LED was turned OFF for 20 seconds to allow the pupil to return to MaxPD; (4) during the last 30 seconds of the session, the MATLAB program actively tracked PD in real-time and modulated the LED intensity to hold the iris as close to MidPD as possible (Supplementary Fig. S1). During this final phase, the system calculated the mean of the PD (MeanPD) once per second and compared it to the MidPD. If MeanPD was 5% above (pupil too dilated = light intensity too low) or below the MidPD (pupil too constricted = light intensity too high), the control code sent a signal to increase or decrease the voltage, respectively. If MeanPD fell very close to MidPD (within 95% to 105% of MidPD), the MATLAB control code continued sending the same voltage to the LED. The MATLAB control code continued performing this analysis until the end of the session. The maximum possible voltage received by the LED during the last 30 seconds of each session was limited to 0.375 V, which corresponded with an LED intensity of 67 lux, to avoid exposing the eye to intense light for extended periods of time.

Image Processing

Custom MATLAB code continuously analyzed a 245 × 330 pixel region of the ANTERION display that displayed an en face camera image of the eye (Supplementary Fig. S2). The system analyzed the PD in real-time throughout the entire scan session (65 seconds) at a rate of five frames per second on average and stored the en face camera image displayed by the ANTERION in a participant-specific folder. Each red, green, blue (RGB) image of the eye was converted into a hue, saturation, and value (HSV) format and then into a grayscale image to facilitate pupil edge detection. The image was then saturated to make the different

gray tones more distinctive and increase image contrast and sharpness. Next, the image was converted into a binary format (black and white pixels). Finally, small white objects in the image (with an area less than 500 pixels) were converted to black pixels to produce a more defined image of the pupil. This process produced a final black and white image with a distinctive black circular shape in the center corresponding to the pupil (see Supplementary Fig. S2). The MATLAB code detected the location and calculated the radius of this post-processed black-and-white image of the pupil in real-time.

It is important to note that while video frames from the live anterior segment OCT (AS-OCT) imaging feed were stored by the custom software at a frequency of five frames per second, these AS-OCT images were not analyzed in this study.

Measurement of PCV and Iris Activity

Data from each imaging session were analyzed offline in MATLAB to calculate two metrics of dynamic iris behavior: peak constriction velocity (PCV) and mid-dilated iris activity (MDIA). PCV was calculated as the maximum change in PD over time during the first constriction phase (t = 6 to 12 seconds; Supplementary Fig. S3). MDIA was defined as the standard deviation (SD) of PD measurements obtained during the last 10 seconds of each session (t = 55 to 65 seconds) relative to the calculated MidPD.

Statistical Analysis

Continuous variables were calculated as means and SDs, and categorical variables were calculated as proportions. Distributions of PCV and MDIA were assessed for normality using the Shapiro-Wilk test. Linear regression analysis was performed between age and PCV or MDIA. A comparative plot (Bland-Altman plot) between MidPD and the mean of the PD during the last 10 seconds of the session was used to assess the agreement between these 2 measurements. The inter-session reproducibility of PCV and MDIA measurements were calculated using intraclass correlation coefficients (ICCs) for randomly selected successful sessions (minimum of 2 successful sessions per participant). The statistical analysis was performed in MATLAB and SPSS statistical software version 28.0 (SPSS Inc., Chicago, IL, USA).

Results

A total of 58 participants were recruited; 14 were non-Hispanic Whites, 19 were Hispanics, 15 were Asian, 1 was Black, and 9 had nonspecific race/ethnicity. One participant (1.72%) was excluded

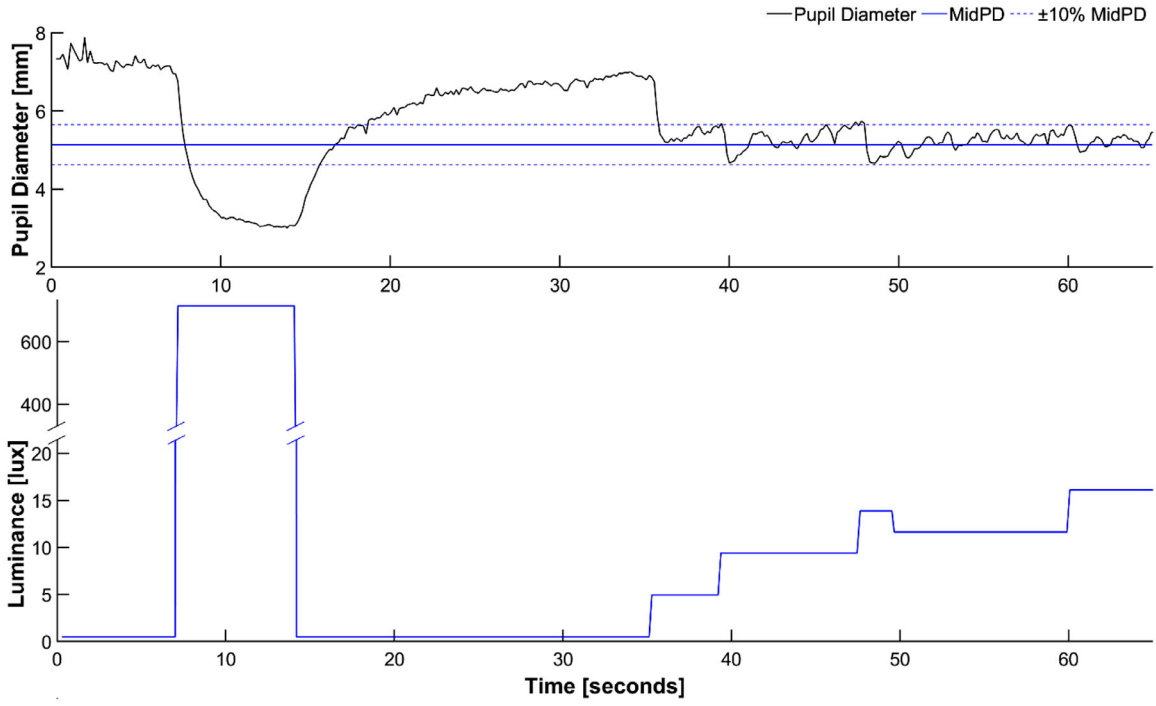

Figure 2. Representative data from a successful 65-second scan session. Changes in pupillary diameter (*top*) and LED light intensity (*bottom*) are shown. MidPD = mid-dilated pupillary diameter.

Table 1. Parameter Measurements of Study Participants, Mean (SD)

Age Range	*N*	PCV, mm/s	MDIA, mm	MaxPD, mm	MinPD, mm	PD Range, mm
<40 y	19	4.47 (0.72)	0.46 (0.17)	6.85 (0.99)	3.31 (0.73)	3.54 (0.83)
40–49 y	5	3.64 (0.67)	0.30 (0.15)	5.98 (1.11)	3.25 (0.58)	2.73 (0.65)
50–59 y	12	3.89 (0.99)	0.38 (0.13)	5.98 (0.95)	3.09 (0.60)	2.89 (0.63)
60–69 y	10	3.51 (0.74)	0.31 (0.12)	4.96 (0.52)	2.89 (0.49)	2.07 (0.32)
>= 70 y	10	3.48 (0.38)	0.28 (0.09)	5.02 (1.07)	2.76 (0.47)	2.26 (0.67)

PCV, peak constriction velocity; MDIA, mid-dilated iris activity; MaxPD, maximum pupil diameter; MinPD, minimum pupil diameter; PD, pupil diameter; SD, standard deviation.

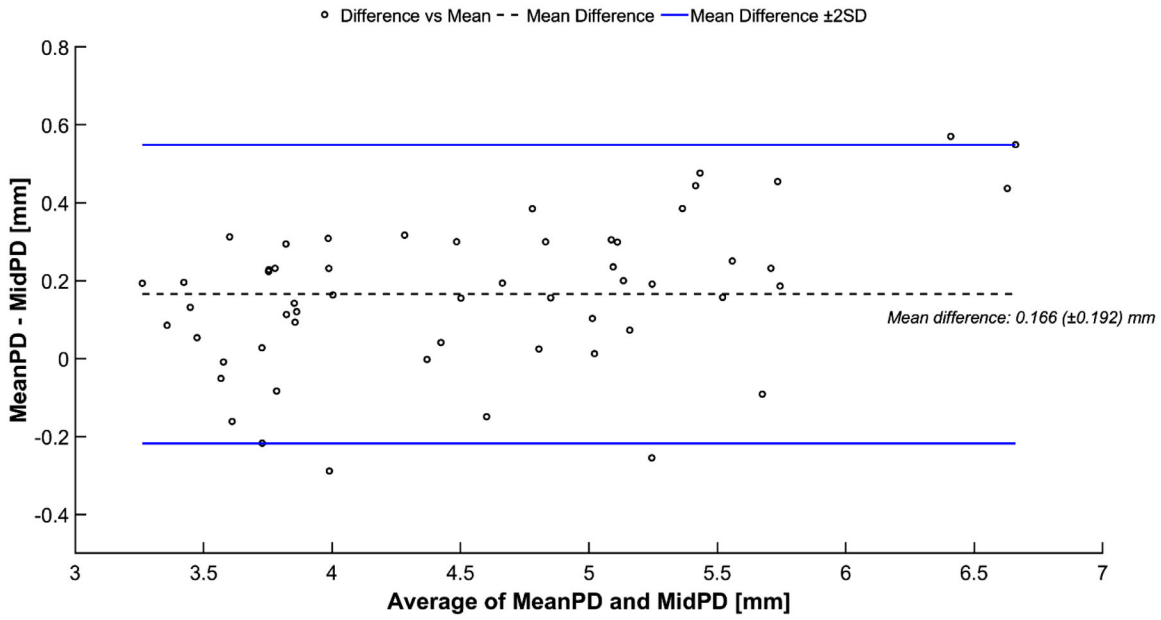

Figure 3. Bland-Altman plot comparing the calculated mid-dilated pupillary diameter (MidPD) and the mean pupillary diameter (PD) during the last 10 seconds of one session eye participant (MeanPD).

due to excessive eye movements during the sessions, and one participant was excluded as none of the three scan sessions was successful. A session was considered successful if the mean PD during the last 10 seconds of the session (MeanPD) fell within 10% (range of 90% to 110%) of MidPD (Fig. 2, top). Based on this definition, 7 participants (12.1%) had 1 successful scan session, 18 participants (31.0%) had 2 successful sessions, and 31 participants (53.4%) had 3 successful sessions. If a participant had more than one successful session (up to 3), only one was randomly selected for the primary analysis.

Fifty-six participants (96.6%) were included in the primary analysis, of whom 32 (55.2%) were women. Mean participant age was 49.8 ± 18.9 years (Table 1). Bland-Altman analysis showed that the difference between the calculated MidPD (target) and observed MeanPD (actual) was relatively consistent for all 56 participants with a mean of 0.166 ± 0.192 mm (Fig. 3).

Mean PCV was 3.92 ± 0.83 mm/s (range = 2.40 to 6.27 mm/s). PCV slowed with older age (Fig. 4). The slope of the linear regression was −0.022 (R^2 = 0.263, $P < 0.001$). Mean MDIA was 0.37 ± 0.15 mm (range = 0.14 to 0.70 mm). MDIA also decreased with older age (Fig. 5). The slope of the linear regression was −0.004 (R^2 = 0.228, $P < 0.001$). PCV for randomly selected successful sessions had an ICC of 0.44 (95% confidence interval [CI] = 0.18–0.64) indicating moderate inter-session reproducibility for this variable. MDIA reproducibility for the same randomly selected successful sessions had an ICC of 0.58 (95%

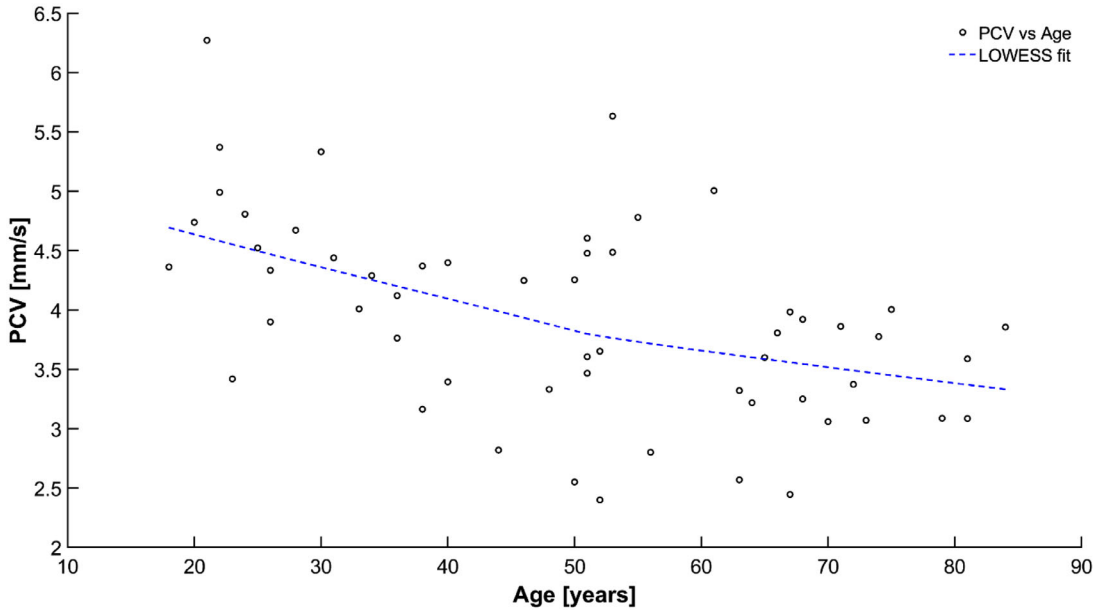

Figure 4. Relationship between peak constriction velocity (PCV) and age. LOWESS regression (*blue dashed line*) shows a negative linear relationship between PCV and age ($P < 0.001$).

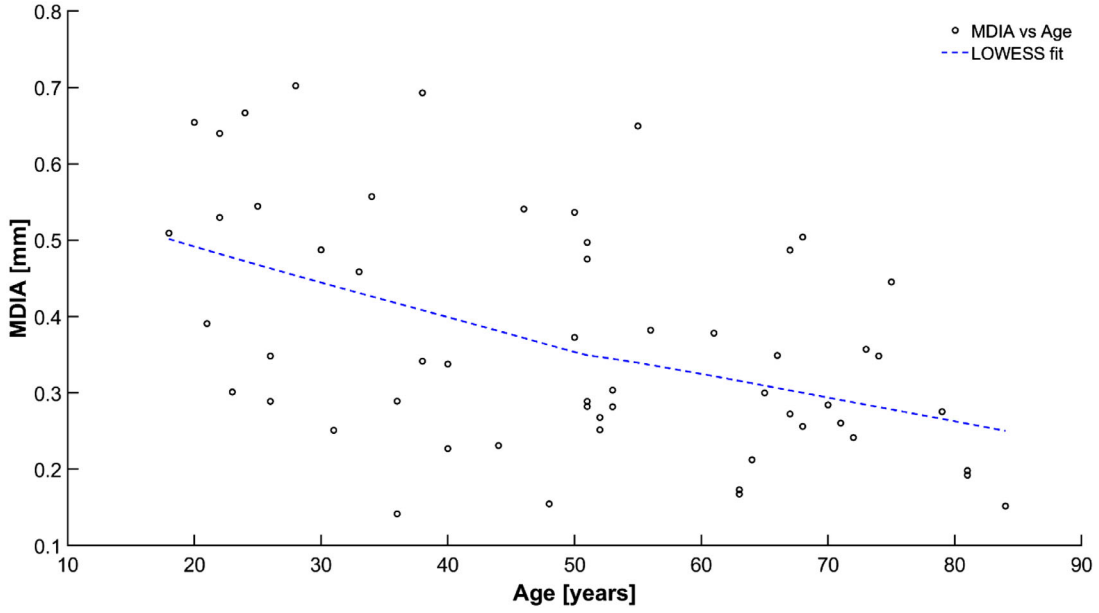

Figure 5. Relationship between mid-dilated iris activity (MDIA) and age. LOWESS regression (*blue dashed line*) shows a negative linear relationship between MDIA and age ($P < 0.001$).

CI = 0.36–0.74) indicating moderate inter-session reproducibility.

A secondary analysis was performed to assess the effect of using a stricter definition of successful session on study findings. In this analysis, a trial was considered successful if the mean PD during the last 10 seconds (MeanPD) of the session fell within 5% (range of 95% to 105%) of MidPD. Forty participants (69.0%) had at least 1 successful session based on this stricter definition, of whom 16 participants (27.6%) had 1 successful scan session, 13 participants (22.4%) had 2 successful sessions, and 11 (19.0%) participants had 3

Table 2. Comparison of Demographic and Biometric Features Between Successful and Unsuccessful Participants and Sessions Using the Stricter Definition of Success

	Mean ± SD or Number		
	Unsuccessful, $n = 18$	Successful, $n = 40$	*P* Value*
Age, y	48.39 ± 20.54	50.70 ± 18.69	0.67
PD dark	6.12 ± 1.47	5.77 ± 1.06	0.32
PD light	3.36 ± 0.83	3.03 ± 0.49	0.07
PD range	2.75 ± 0.89	2.74 ± 0.87	0.96
MDIA	0.60 ± 0.28	0.30 ± 0.12	**<0.01**
PCV	3.93 ± 1.19	3.94 ± 0.77	0.96
MidPD	4.72 ± 1.10	4.37 ± 0.69	0.15
Gender, male/female	4/14	20/20	
Race			
Asian	5	10	
Black		1	
Hispanic	7	12	
White	3	11	
Not specified	3	6	

*T-test.

successful sessions. The only significant difference in demographics and biometrics between the participants with and without a successful session was that unsuccessful participants had significantly greater MDIA (Table 2).

Results from the secondary analysis were resembled results from the primary analysis despite fewer participants and sessions meeting the definition of success. Mean participant age was 50.0 ± 18.7 years (Supplementary Table S1). Mean PCV was 3.94 ± 0.76 mm/s, and mean MDIA was 0.30 ± 0.12 mm. Bland-Altman plot showed a mean difference between the calculated MidPD and observed MeanPD of 0.07 ± 0.13 mm (Supplementary Fig. S4). The slope of the linear regression between PCV and age was −0.02 ($R^2 = 0.19$, $P = 0.005$; Supplementary Fig. S5). The slope of the linear regression between MDIA and age was −0.003 ($R^2 = 0.22$, $P = 0.002$; Supplementary Fig. S6). PCV for randomly selected successful sessions had an ICC of 0.65 (95% CI = 0.35–0.83). MDIA reproducibility for the same randomly selected successful sessions had an ICC of 0.51 (95% CI = 0.14–0.75).

Discussion

In this study, we developed a programmable closed-loop iris control system to track, modulate, and assess dynamic iris behavior. The system tracks PD in real-time through automated analysis of en face camera images, allowing it to modulate PD dynamically and maintain the iris in a mid-dilated position. We tested the system by assessing the relationship between age and dynamic iris behavior, establishing that PCV and MDIA decrease with older age. This system represents a flexible tool for studying the role of dynamic iris behavior in ocular disease, including elucidating anatomic mechanisms of AAC and identifying dynamic risk factors for PACG.

In the first portion of each scan session, the maximally dilated pupil is brought to the maximally constricted position using a bright stimulus and then allowed to dilate back to maximally dilated position once the stimulus is turned off. This portion has two functions; it allows for (1) measurement of MinPD and MaxPD to calculate MidPD and (2) measurement of constriction and dilation velocities to assess their role as risk factors in PACD. MidPD is important as the risk of AAC is believed to be highest when the iris is in the mid-dilated position. The role of PCV as a risk factor in PACD has previously been reported; PCV is slower in eyes with angle closure than in eyes with open angles.[14] This slowing may reflect greater lens-iris contact or aberrant biomechanical properties of the iris. However, little is known about the relationship between peak or average dilation velocity and PACG risk, perhaps because dilation occurs more slowly and is more difficult to quantify. Therefore, more thorough analysis of data from this

portion of the scan session may be beneficial in future studies on vector forces during constriction and dilation.[13]

In the second portion of each scan session, the system calculates the MidPD value and modulates a dim stimulus to maintain the iris in the mid-dilated position. The system achieves this using a negative feedback algorithm that reads the current PD, compares it with the desired size of MidPD, and changes the output voltage and LED intensity accordingly to approximate the MidPD value. The clinical significance of the mid-dilated position in angle closure eyes is widely accepted, especially as a risk factor for AAC. Pupillary block is thought to be exacerbated in the mid-dilated position due to increased iris-lens contact and resistance to aqueous flow.[15] Furthermore, a mid-dilated pupil is a classic examination finding in cases of AAC.[16] Although these findings suggest that the mid-dilated position plays an important role in dynamic disease mechanisms, this has never been demonstrated experimentally, as AAC attacks are exceedingly rare and difficult to predict.[17,18] The capability of our system to maintain the iris in the mid-dilated position, together with built-in AS-OCT functionality, could provide researchers with an important tool to study and understand the effects of iris dynamics that contribute to anatomic mechanisms of AAC.

We tested the iris control system by characterizing the effect of age on dynamic iris behavior, which appears to decrease linearly with older age. Our results show that PCV decreases linearly with older age, which is consistent with previous studies that reported decreased pupillary diameter, amplitude, and constriction and dilation velocities in elderly individuals.[19,20] These changes are likely due to decreased sympathetic activity with increasing age, which affects static PD and the pupillary light reflex.[19] In addition, MDIA, which reflects how closely the system was able to hold the iris at the calculated MidPD, also decreases linearly with older age, indicating that the irises of older individuals tend to exhibit less activity in the mid-dilated state when compared with younger ones. Intuitively, this could reflect increased iris-lens contact and contribute to greater risk of pupillary block under specific environmental conditions. These observations are consistent with widely held theories on the pathogenesis of AAC, and older age is a well-established risk factor for PACD of all severities.[21-23] However, quantitative biometric analysis of AS-OCT images will be needed to establish the relationship between the mid-dilated position and dynamic changes in pupillary block.

We found substantial intra- and interindividual variability in dynamic iris behavior that exceeds variability among static AS-OCT measurements of iris parameters.[24,25] There are several reasons to believe this observation more likely reflects intrinsic variability of dynamic iris behavior than extrinsic variability introduced by the iris control system. First, we tested two definitions of success; the system was able to hold MeanPD within 10% of MidPD for 96% of participants and within 5% of MidPD for 69% of participants. When we compared demographic and biometric parameters between successful and unsuccessful sessions for the stricter definition of success, MDIA was the only parameter with a significant difference. This suggests that some individuals exhibit greater amounts of iris activity in the mid-dilated position that makes it difficult to hold MeanPD within a narrow PD window. Second, interindividual reproducibility was moderate for PCV and MDIA, despite PCV being a relatively simpler pupillary response. This suggests that responses of the iris to external stimuli are variable and multifactorial, even when changes in lighting are fixed and unidirectional (e.g. dark to light). Finally, there was high interindividual variability in MDIA despite the system operating under the same feedback algorithm and narrow window of light intensity for each participant. Whereas these findings do not remove the possibility that extrinsic, system-level variability contributes to dynamic iris behavior, they suggest that intrinsic, participant-level variability plays a larger role.

Our iris control system, which is in its first iteration, has several limitations. First, the system did not always achieve and maintain the MidPD. In some cases, the iris had large responses to small incremental changes in light intensity, consistent with physiologic hippus.[26] These rapid and wide fluctuations in PD made it difficult for the system to make appropriate adjustments in voltage output to counteract the changes. Fortunately, hippus decreases with age; therefore, it is less likely to affect studies on PACD, which tends to be a disease of the elderly. In other cases, the voltage that controlled the LED intensity was insufficient to constrict the pupil to within 10% of the MidPD. Therefore, a dynamic voltage step could be beneficial in future iterations of the feedback algorithm. Second, the time required by the system to achieve the MidPD was relatively long, taking around 20 seconds in some cases. This time could be reduced by using a more dynamic algorithm that adjusts voltage increments based on dynamic factors, such as participant age or dilation and constriction velocities. Therefore, further work is needed to optimize the system and identify determinants of dynamic iris behavior.

In summary, we developed and tested a programmable closed-loop iris control system for modulating and studying dynamic iris behavior under precisely controlled lighting conditions. This system represents a novel method to perform real-time analysis of PD and control iris behavior, including maintaining the mid-dilated position. The system concurrently stores en face camera and cross-sectional AS-OCT images during each scan session and store them for offline analysis. Although AS-OCT images were not analyzed in this study, quantitative analysis of these images could help identify novel risk factors for angle closure or provide information about biomechanical properties of ocular tissues, such as the iris, that play a role in disease pathogenesis.[16,27,28] In the future, this system could be used to study determinants of dynamic iris behavior, elucidate mechanisms of acute and chronic angle closure, and compare iris dynamics between eyes with and without PACD to identify novel disease risk factors.

Acknowledgments

Supported by grants K23 EY029763 from the National Eye Institute, National Institute of Health, Bethesda, Maryland; a Young Clinician Scientist Research Award from the American Glaucoma Society; and an unrestricted grant to the Department of Ophthalmology from Research to Prevent Blindness, New York, NY.

Disclosure: **G. Apolo**, None; **N. Lazkani**, None; **S. Zhou**, None; **A.E. Song**, None; **A.A. Pardeshi**, None; **L. Torossian**, None; **K. Nguyen**, None; **R.N. Weinreb**, None; **B.Y. Xu**, None

References

1. Cheung CYL, Liu S, Weinreb RN, et al. Dynamic analysis of iris configuration with anterior segment optical coherence tomography. *Invest Ophthalmol Vis Sci*. 2010;51(8):4040–4046.
2. Wang BS, Narayanaswamy A, Amerasinghe N, et al. Increased iris thickness and association with primary angle closure glaucoma. *Br J Ophthalmol*. 2011;95(1):46–50.
3. Wang B, Sakata LM, Friedman DS, et al. Quantitative Iris Parameters and Association with Narrow Angles. *Ophthalmology*. 2010;117(1):11–17.
4. da Soh Z, Thakur S, Majithia S, Nongpiur ME, Cheng CY. Iris and its relevance to angle closure disease: A review. *Br J Ophthalmol*. 2021;105(1):3–8.
5. Xu BY, Lifton J, Burkemper B, et al. Ocular Biometric Determinants of Anterior Chamber Angle Width in Chinese Americans: The Chinese American Eye Study. *Am J Ophthalmol*. 2020;220:19–26.
6. Lifton J, Burkemper B, Jiang X, et al. Ocular Biometric Determinants of Dark-to-Light Change in Angle Width: The Chinese American Eye Study. *Am J Ophthalmol*. 2022;237:183–192.
7. Xu BY, Friedman DS, Foster PJ, et al. Ocular Biometric Risk Factors for Progression of Primary Angle Closure Disease: The Zhongshan Angle Closure Prevention Trial. *Ophthalmology*. 2022;129(3):267–275.
8. Quigley HA, Silver DM, Friedman DS, et al. Iris Cross-Sectional Area Decreases With Pupil Dilation and Its Dynamic Behavior Is a Risk Factor in Angle Closure. *J Glaucoma*. 2009;18(3):173–179.
9. Crowell EL, Chuang AZ, Bell NP, Blieden LS, Feldman RM. Using Anterior Segment Optical Coherence Tomography (ASOCT) Parameters to Determine Pupillary Block Versus Plateau Iris Configuration. *J Glaucoma*. 2020;29(11):1036–1042.
10. Woo EK, Pavlin CJ, Slomovic A, Taback N. Ultrasound Biomicroscopic Quantitative Analysis of Light-Dark Changes Associated With Pupillary Block. *Am J Ophthalmol*. 1999;127(1):43–47.
11. Zhang X, Liu Y, Wang W, et al. Why does acute primary angle closure happen? Potential risk factors for acute primary angle closure. *Survey of Ophthalmol*. 2017;62(5):635–647.
12. Zhang Y, Li SZ, Li L, He MG, Thomas R, Wang NL. Dynamic iris changes as a risk factor in primary angle closure disease. *Invest Ophthalmol Vis Sci*. 2016;57(1):218–226.
13. Zheng C, Cheung CY, Aung T, et al. In vivo analysis of vectors involved in pupil constriction in Chinese subjects with angle closure. *Invest Ophthalmol Vis Sci*. 2012;53(11):6756–6762.
14. Zheng C, Cheung CY, Narayanaswamy A, et al. Pupil dynamics in Chinese subjects with angle closure. *Graefe's Arch Clin Exp Ophthalmol*. 2012;250(9):1353–1359.
15. Aptel F, Denis P. Optical Coherence Tomography Quantitative Analysis of Iris Volume Changes after Pharmacologic Mydriasis. *Ophthalmology*. 2010;117(1):3–10.
16. Leung CKS, Cheung CYL, Li H, et al. Dynamic analysis of dark-light changes of the anterior chamber angle with anterior segment OCT. *Invest Ophthalmol Vis Sci*. 2007;48(9):4116–4122.

17. He M, Jiang Y, Huang S, et al. Laser peripheral iridotomy for the prevention of angle closure: a single-centre, randomised controlled trial. *The Lancet*. 2019;393(10181):1609–1618.
18. Baskaran M, Kumar RS, Friedman DS, et al. The Singapore Asymptomatic Narrow Angles Laser Iridotomy Study: Five-Year Results of a Randomized Controlled Trial. *Ophthalmology*. 2022;129(2):147–158.
19. Bitsios P, Prettyman R, Szabadi E. *Changes in Autonomic Function with Age: A Study of Pupillary Kinetics in Healthy Young and Old People*. Vol. 25; 1996. Available at: https://academic.oup.com/ageing/article/25/6/432/14188.
20. Telek HH. The Effects of Age Pupil Diameters at Different Light Amplitudes. *Beyoglu Eye Journal*. 2018;3(2):80–85.
21. Liang Y, Friedman DS, Zhou Q, et al. Prevalence and characteristics of primary angle-closure diseases in a rural adult Chinese population: The Handan eye study. *Invest Ophthalmol Vis Sci*. 2011;52(12):8672–8679.
22. Sawaguchi S, Sakai H, Iwase A, et al. Prevalence of primary angle closure and primary angle-closure glaucoma in a southwestern rural population of Japan: The Kumejima study. *Ophthalmology*. 2012;119(6):1134–1142.
23. Yamamoto T, Iwase A, Araie M, et al. The Tajimi study report 2: Prevalence of primary angle closure and secondary glaucoma in a Japanese population. *Ophthalmology*. 2005;112(10):1661–1669.
24. Pardeshi AA, Song AE, Lazkani N, Xie X, Huang A, Xu BY. Intradevice repeatability and interdevice agreement of ocular biometric measurements: A comparison of two swept-source anterior segment oct devices. *Transl Vis Sci Technol*. 2020;9(9):1–9.
25. Xu BY, Mai DD, Penteado RC, Saunders L, Weinreb RN. Reproducibility and Agreement of Anterior Segment Parameter Measurements Obtained Using the CASIA2 and Spectralis OCT2 Optical Coherence Tomography Devices. *Journal of Glaucoma*. 2017;26(11):974–979.
26. Howarth PA, Heron G, Greenhouse DS, Bailey IL, Berman SM. Discomfort from glare: The role of pupillary hippus. *Lighting Research and Technology*. 1993;25(1):37–42.
27. Narayanaswamy A, Nai MH, Nongpiur ME, et al. Young's modulus determination of normal and glaucomatous human Iris. *Invest Ophthalmol Vis Sci*. 2019;60(7):2690–2695.
28. Panda SK, Tan RKY, Tun TA, et al. Changes in iris stiffness and permeability in primary angle closure glaucoma. *Invest Ophthalmol Vis Sci*. 2021;62(13):29.